Effect of alkali promoters (K) on nitrous oxide abatement over Ir/Al$_2$O$_3$ catalysts

E. Papista[1,*], E. Pachatouridou[2,3], M.A. Goula[4], G.E. Marnellos[1,2,5], E. Iliopoulou[2], M. Konsolakis[3] and I.V. Yentekakis[6]

[1]Department of Mechanical Engineering, University of Western Macedonia, GR-50100 Kozani, Greece

[2]Chemical Process and Energy Resources Institute (CPERI),Centre for Research and Technology Hellas (CERTH), GR-57001 Thermi, Thessaloniki, Greece

[3]School of Production Engineering and Management, Technical University of Crete, GR-73100 Chania, Crete, Greece

[4]Department of Environmental and Pollution Control Engineering, Technological Educational Institute of Western Macedonia (TEIWM), GR – 50100, Koila, Kozani, Greece

[5]Department of Environmental Engineering, University of Western Macedonia, GR-50100, Kozani, Greece

[6]School of Environmental Engineering, Technical University of Crete, GR-73100 Chania, Crete, Greece

*Corresponding author: epapista@uowm.gr

Abstract

The promoting impact of potassium (0-1 wt. % K) on nitrous oxide (N_2O) catalytic decomposition over Ir/Al_2O_3 is investigated under both oxygen deficient and oxygen excess conditions. All samples were characterized by means of X-ray powder diffraction (XRD), temperature-programmed reduction (H_2-TPR), ammonia desorption (NH_3-TPD) and Fourier Transform Infrared Spectroscopy of pyridine adsorption (FTIR-Pyridine). The results reveal that the K-free Ir/Al_2O_3 catalyst consists mainly of the IrO_2 phase, exhibiting also significant Lewis acidity, which is gradually eliminated by the addition of K. Catalytic performance results showed that the deN_2O performance in the absence of O_2 in the feed mixture is negatively affected upon increasing potassium loading. However, under oxygen excess conditions, a pronounced effect of K is observed. Although the catalytic performance of the un-doped catalyst is drastically hindered by the presence of O_2, the K-promotion notably prohibits the oxygen poisoning. The optimum deN_2O performance is obtained with potassium loading of 0.5 wt. % K, which offers complete conversion of N_2O at 580° C, instead of the corresponding 50% N_2O conversion achieved with the un-modified sample.

Keywords: N_2O decomposition, Iridium, Potassium promoter, Alumina

1. Introduction

Nitrogen oxides abatement is a subject of major environmental importance. Most of the environmental protection efforts have been devoted to nitric oxides (NOx) abatement, which are recognized as an important precursor of acid rain, also responsible for the formation of photochemical smog. However, recently a lot of academic and policy attention has been focused on the N_2O emissions control [1]. Nitrous oxide (N_2O) is listed as one of the most harmful greenhouse gases with a strong global warming potential (310 times higher than that of CO_2), that severely contributes to the stratospheric ozone layer depletion [2]. N_2O is emitted by both natural and anthropogenic sources, whereas the largest portion of nitrogen oxides emissions is attributed to human activities, including fuels combustion in stationary and mobile sources, agricultural activities and industrial processes. In relation to the contribution of mobile applications to N_2O emissions, automobiles are among the most significant sources. N_2O is a by-product of reactions taking place in Three-Way Catalytic converters (TWCs), being notably affected by operation temperature, washcoat composition and aging. Real-time data clearly show that N_2O emissions are primarily formed during the ''cold start'' and ''intermediate temperature'' periods. For this reason, mitigation of N_2O is an issue of substantial environmental concern [3, 4]. Although several methods have been proposed for the abatement of nitrous oxide, the direct catalytic decomposition of N_2O to N_2 has been proved as the most promising after-treatment technique for N_2O removal from exhaust gases [5, 6].

The catalytic decomposition of N_2O to molecular nitrogen and oxygen has been investigated over a wide variety of catalysts, involving mainly noble metal supported catalysts, metal oxides and ion-exchanged zeolites. Among the catalysts that have been studied so far for the decomposition of nitrous oxide, the noble metals (Rh, Pt, Pd etc.) exhibit satisfactory activity, even at low temperatures. However, their high cost in combination with the inhibiting effect of O_2, H_2O and SO_2 that coexist in the exhaust gases, render their practical application unadvisable. Thus, research efforts are focused on the enhancement of their catalytic properties-towards the decrease of precious metal loading and the improvement of their tolerance-through the utilization of structural (e.g. rare earth oxides) and/or surface (e.g. alkalis) promoters [5, 7-13].

Recently particular emphasis is given on the modification of catalyst surface chemistry, which can be achieved directly by means of electropositive surface promoters, such as alkalis or alkaline earths [7-14]. Taking into consideration that an important factor of promotion in catalysis is the electrostatic interactions in the double layer developed at the catalyst-gas interface [15], a possible explanation for the electronic mode of action of electropositive promoters is the strengthening of metal-electron accepting adsorbates (e.g. N_2O, NO, CO) bond, leading to the enhancement of their adsorption [16]. In the case of N_2O catalytic decomposition, the beneficial effect of alkali promotion in de-N_2O activity lies in the fact that alkali addition creates an electron enriched metal surface that causes a strengthening of the metal-N_2O adsorption bond, thus favoring its dissociative chemisorption [17-20]. Under this view, it has been demonstrated that the addition of Li, Na K, Cs or Sr on Rh/Al_2O_3 catalyst, increased the efficiency of the catalyst for the nitrous oxide abatement [13, 21]. In addition, K-modification (either electrochemically or conventionally) on Pd/Al_2O_3 catalysts enhanced the N_2O decomposition in the presence of hydrocarbons [11, 13, 22].

Our previous study [23] revealed that among Pt, Pd and Ir alumina supported catalysts, the Ir-based catalysts demonstrated the highest deN_2O performance, even at low metal loadings (0-1 wt.% Ir). However, the inhibition induced by the presence of excess oxygen in the feed, teased our interest to investigate the impact of alkali promoters (K) on the physicochemical properties and catalytic performance of Ir/Al_2O_3 catalysts towards the N_2O decomposition. In this context, the as prepared catalysts were characterized *via* several complementary techniques to gain insight into the impact of K promoter on the deN_2O performance.

2. Experimental

2.1 Materials

The preparation of Al_2O_3 support was carried out using the precipitation method. $Al(NO_3)_3 \cdot 9H_2O$ (98.5% pure, supplied by Chem-Lab) was employed as the precursor salt. A precipitating agent (NH_3, 25v/v %) was added at room temperature to a continuously stirred solution of the precursor material, until the pH was stabilized at ~10 (for 3 h). The resulting precipitate was filtered, dried overnight at 110°C and calcined at 600°C for 2 h under air flow.

The addition of the active phase (Ir) and alkali promoter (K) was conducted sequentially using the dry impregnation method. First, the incorporation of iridium (0.5 wt. %) to alumina support took place, using an aqueous solution of $IrCl_3 \cdot H_2O$ (98% pure, supplied by Merck). The derived sample was dried overnight at 100°C and calcined at 600°C for 3 h under air flow. Secondly, the potassium was added, using KNO_3 (99% pure, supplied by Strem Chemicals) as the precursor material, with the appropriate concentrations in order to achieve the desirable loading, varying between 0-1 wt%. An identical impregnation procedure was followed as before. The resulted suspension was dried and calcined according to the previous temperature program. The as prepared samples are herein labeled as Ir(xK)/Al, where x is the potassium loading (x= 0, 0.25, 0.50 and 1.00 wt. % K).

2.2 Catalysts Characterization

2.2.1 Textural Characterization (BET, ICP)

The physicochemical characteristics of the as prepared catalysts were determined by the adsorption–desorption isotherms at -196°C, using the Nova 2200e (Quantachrome) flow apparatus. BET surface areas were obtained according to the Brunauer–Emmett–Teller (BET) method, at the relative pressure in the range of 0.05–0.30. The total pore volume was calculated based on nitrogen volume at the highest relative pressure, whereas the average pore size diameter was determined by the Barrett-Joyner-Halenda (BJH) model, using the desorption branch of the isotherm. Prior to measurements the samples were degassed at 350°C for 5 h under vacuum.

2.2.2 Structural Characterization (XRD)

The crystalline structure of the catalysts was determined by X-ray powder diffraction (XRD) on a Siemens D 500 diffractometer at 40 kV and 30 mA, with Cu K_α radiation (λ=0.154 nm). Diffractograms were recorded in the 2θ=2-80° range at a scanning rate of 0.02^o over 2 s. The Scherrer equation was employed, where applicable, to determine the particle size of different phases, based on their most intense diffraction peaks.

2.2.3 Redox Characterization (H_2-TPR)

Temperature-programmed reduction with hydrogen (H_2-TPR) was performed by loading 100 mg of catalytic sample in a quartz fixed bed reactor, coupled with mass spectrometry (MS). During experiments the catalyst was exposed to a 5v/v % H_2/He mixture at a total flow rate of 50 cm^3/min. Reactor temperature was programmed to start from ambient temperature and ramp up to 700°C, at a rate of 5°C/min. The influent and effluent gases were analyzed by mass spectrometry (MS). The main m/z fragment registered was H_2=2. Samples were pre-treated at 300°C (with a heating rate of 3°C/min) for 1 h under He flow to remove water and any other possible physisorbed species and then cooled down to room temperature in the same atmosphere before the TPR spectra acquisition.

2.2.4 Acidity Measurements (NH_3-TPD, FTIR-Pyridine)

The measurement of the catalysts acidity was performed *via* ammonia temperature-programmed desorption (NH_3-TPD) and FTIR studies of pyridine adsorption (FTIR-Pyr). NH_3-TPD was conducted on the same apparatus with the TPR measurements. A catalyst mass of 100 mg was loaded in a quartz fixed bed reactor. Prior to the measurement, a pretreatment under pure He flow took place at 500°C (with a heating rate of 3°C/min) for 1 h. The sorption of NH_3 was conducted by exposing the catalyst sample to a 5v/v% NH_3/He at 100°C for 1 h. The gaseous or physisorbed NH_3 was removed by purging with a He flow at 100°C for 1 h. Then the sample was heated to 700°C with a ramp of 10°C/min. The desorbed NH_3 was monitored continuously via mass spectrometry. The main m/z fragment registered was NH_3=15.

For the Fourier Transform Infrared Spectroscopy (FTIR-Pyridine) experiment, the IR spectra were collected with a resolution of 4cm^{-1}, using a Nicolet 5700 spectrometer equipped with a homemade stainless steel IR cell with CaF_2 windows. The infrared cell, loaded with self-supporting wafers (~15mg/cm^2), is connected to a high vacuum line consisting of turbomolecular and diaphragm pumps; both sample holder and vacuum line are heated to avoid pyridine condensation. Before IR spectra acquisition, samples were heated at 450°C under vacuum (10^{-6} mbar) for 1 h to desorb any physisorbed species. Then the reference spectrum of each sample is collected at 150°C. Spectra of adsorbed pyridine were obtained at 150°C and 1 mbar by equilibrating the catalyst wafer with the probe vapour, added in pulses for 1 h. In order to evaluate the strength of the acid sites, three more spectra were collected at 250ºC, 350ºC and 450ºC, representing the weak, medium and strong acid sites. The concentration of acid sites was calculated using the Lambert-Beer's law and the appropriate molar extinction coefficients. Pyridine adsorption shows

two bands; one at 1450 cm^{-1} attributed to pyridine coordinated to Lewis sites and a second one at 1545 cm^{-1} assigned to protonated pyridine on Brönsted acid sites. These bands are considered as most representative for the quantification of Lewis and Brönsted acid sites [24-26].

2.3 Catalytic Activity Measurements

Catalytic performance experiments were carried out in a tubular, quartz fixed-bed reactor, with an inner diameter of 8 mm. The reactor loading was 100 mg, diluted with 50 mg of SiC, while the total gas flow feed rate was 150 cm^3 (STP)/min corresponding to a Gas Hourly Space Velocity (GHSV) of 40000 h^{-1}. The feed composition during N_2O catalytic decomposition experiments was either 0.1v/v% N_2O (absence of O_2) or 0.1v/v% N_2O and 2v/v% O_2 (presence of O_2), balanced with He. Before catalytic evaluation measurements, all catalyst samples were pretreated in pure He flow (100 cm^3/min) for 1 h at 600°C. The N_2O conversion performance was evaluated in the temperature range of 200-600°C. The composition of the produced gas stream was analyzed by a gas chromatograph (Shimadzu 14B) equipped with a Porapak QS and a molecular sieve 5A columns. The only products detected during the N_2O decomposition reaction under the experimental conditions employed, either in the presence or absence of O_2, were N_2 and O_2.

3. Results and Discussion

3.1 Catalysts Characterization Results

The textural characteristics of the as prepared catalysts are presented in Table 1. A slight decrease, due to the employed low metal loadings, in the total surface area is observed upon the addition of iridium on alumina support and even less upon the addition of potassium. This decrease is probably related with the blockage of support pores by iridium and potassium metals as well as to the additional calcination procedure that follows the impregnation of the metals.

Table 1. Textural characteristics of catalytic materials.

Catalyst code	K content (wt.%)	K/Ir atomic ratio	S_{BET} (m^2/ g)	Pore Volume (cm^3/ g)	Av. Pore Diameter (nm)	TPR Peaks (°C)[a]
Al_2O_3	0	0	179.6	0.36	8.1	-
Ir(0K)/Al	0	0	160.3	0.34	8.6	233
Ir(0.25K)/Al	0.25	2.46	155.8	0.34	8.7	238
Ir(0.5K)/Al	0.50	4.92	153.3	0.35	9.1	245
Ir(1K)/Al	1.00	9.84	153.6	0.34	8.9	253

[a] Indicated by H_2-TPR experiments

Catalysts characterization *via* XRD and H_2-TPR techniques revealed that the dominant phase of iridium on K-free catalyst is IrO_2. According with the XRD patterns of Figure 1, the presence of IrO_2 is clearly evidenced from the characteristic diffraction peaks at 28°, 34.7° and 54° (2θ) [27]. The formation of iridium oxide phase was also confirmed by H_2-TPR experiments, which revealed a well-defined reduction peak at 233°C, attributed to the reduction of Ir oxide phase (Table 1) [28].
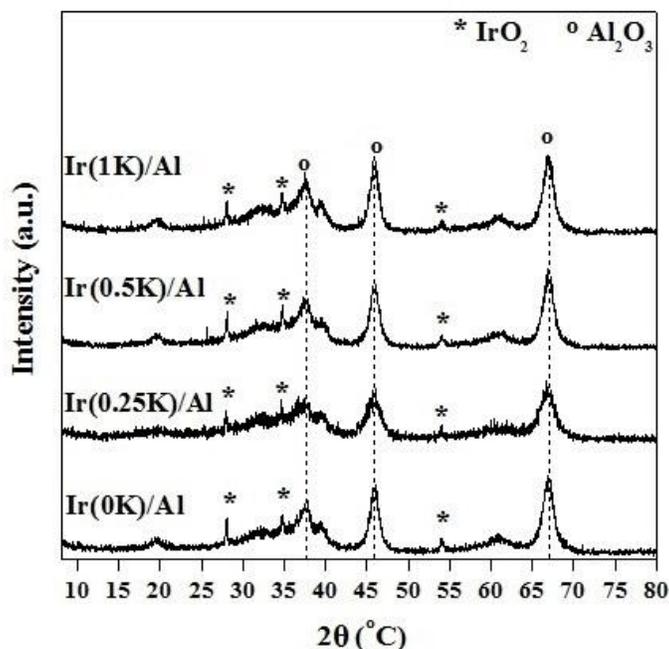

Figure 1. XRD patterns of K-free and K-doped Ir/Al catalysts.

Interestingly, the reduction temperature of the metal oxide phase (IrO_2) shifts to higher temperatures with the increase of K content (Table 1). An upward shift of reduction temperature by about 10°C and 20°C was obtained by doping with 0.5 and 1.0 wt. % K, respectively. A similar trend was reported in the case of K-modified Fe-Cu based catalysts [29], where the addition of the potassium suppressed the reduction of iron and copper, shifting the reduction temperature of all metal oxide species to higher temperatures. On the same direction Vernoux *et al.* [30] found, by means of oxygen TPD experiments, that the temperature of the oxygen desorption peak is shifted upward upon increasing Na promoter loading on Pt/Al_2O_3 catalysts. Therefore the increase in reduction temperature of iridium oxides in the present case, most probably reflects a strengthening in the Ir-O bond due to K interaction with iridium particles (note that oxygen is an electron acceptor adsorbate [31]). The XRD patterns of Ir(K)/Al samples did not reveal any new peak related to K. Only a small decrease of the intensities of IrO_2 phase was observed, in relation to the un-promoted sample.

Figure 2 shows the NH_3-TPD profiles of K-free and K-doped Ir/Al catalysts. The K-free catalyst exhibits a desorption peak of NH_3 at around 370°C, which can be ascribed to Lewis acid sites. The latter is further

confirmed by the FTIR-pyridine results, presented below. The addition of 0.25 wt. % K shifts this peak to a lower temperature (~300°C), indicating that the strength of surface acid sites is notably decreased by potassium. Further increase of the potassium loading (0.50-1.00 wt. %), resulted in a significant attenuation of Lewis acid sites.
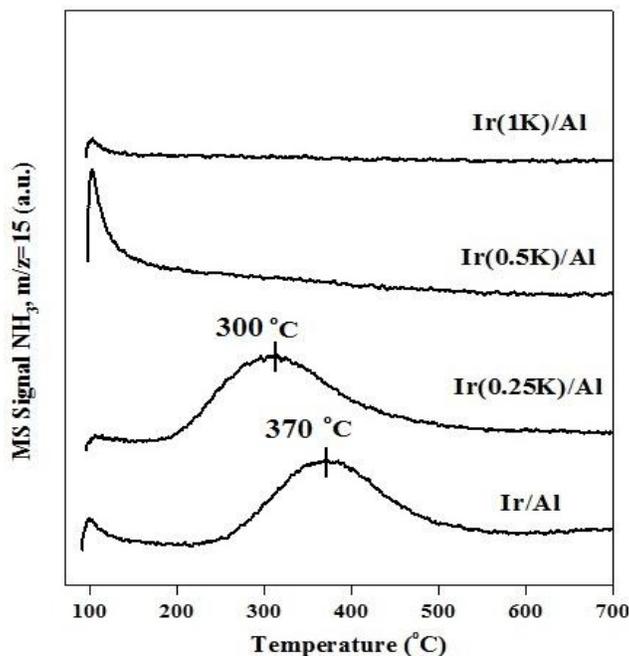

Figure 2. NH$_3$-TPD profiles of K-free and K-doped Ir/Al catalysts.

However, the assessment of the catalysts acidity *via* FTIR-pyridine can provide a more accurate estimation of surface acidity. Pyridine in gas phase is stronger than ammonia, according with their proton affinities values (PA$_{PYR}$=922.2 kJ/mol, PA$_{NH3}$=857.7 kJ/mol), thus allowing the discrimination of very weak Lewis acid sites [32]. Table 2 presents the concentrations of the surface acidity for all catalysts, as well as the discrimination of the acidity to very weak, weak, medium and strong acid sites, as estimated by the FTIR-pyridine measurements. All the catalysts presented only Lewis and no Brönsted acidity. K-free Ir/Al catalyst exhibits significant Lewis acid sites (115 μmol/g), with a high concentration of strong acid sites (25.9 μmol/g). The addition of K is detrimental for the Lewis acidity, as also observed by NH$_3$-TPD. At high K loadings (0.50-1.00 wt. %), the level of strong acid sites is decreasing by more than 90% in comparison with the un-doped sample. Interestingly, an almost linear decrease in acidity is obtained upon increasing K loading. These findings are in agreement with previous studies, reporting that alkaline ions increase the basic strength of catalyst surface while eliminating the Lewis acidity [11, 33-35].

Table 2. Acidity of K-free and K-doped Ir/Al catalysts .

Catalyst code	Strength of Lewis Acid Sites (µmol/g)[a]				Total Lewis Acidity (µmol/g)[a]
	Very Weak	Weak	Medium	Strong	
Ir(0K)/Al	41.3	30.2	17.6	25.9	115.0
Ir(0.25K)/Al	47.7	25.2	12.7	8.7	94.3
Ir(0.5K)/Al	36.2	21.3	8.4	2.5	68.4
Ir(1K)/Al	25.3	7.5	1.0	1.9	35.7

[a] Estimated by FTIR-Pyridine experiments

3.2 Effect of Potassium addition on Catalysts Activity

The effect of electropositive promoters on the de-N_2O behavior of Ir/Al_2O_3 catalysts was studied in typical light-off experiments, both in the absence (Fig. 3) and in the presence of excess oxygen (Fig. 4). The catalytic results, in the absence of O_2, show that the de-N_2O performance is hindered upon increasing potassium loading.
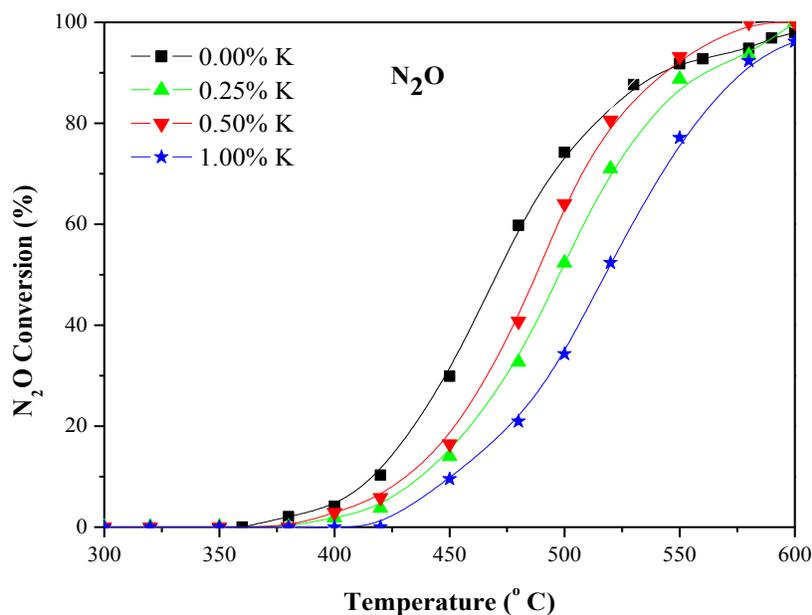

Figure 3. N_2O conversion over Ir(K)/Al catalysts in the absence of O_2 (GHSV: 40000h^{-1}, Feed: 0.1 v/v% N_2O diluted in He)

However, in the case of N_2O decomposition under excess oxygen conditions, a completely different behavior is observed. Despite the fact that the catalytic performance of the un-promoted Ir/Al_2O_3 catalyst is

drastically hindered by the presence of O_2, it is revealed that the addition of the electropositive promoter improves the catalytic efficiency, shifting the conversion profiles to lower temperatures. A superior behavior is offered by Ir(0.5K)/Al$_2$O$_3$ catalyst, while higher potassium loadings (1.0 wt.%) have a detrimental effect on N$_2$O conversion. The latter implies an optimum promoter loading at 0.5 wt.% K. (Fig. 4).
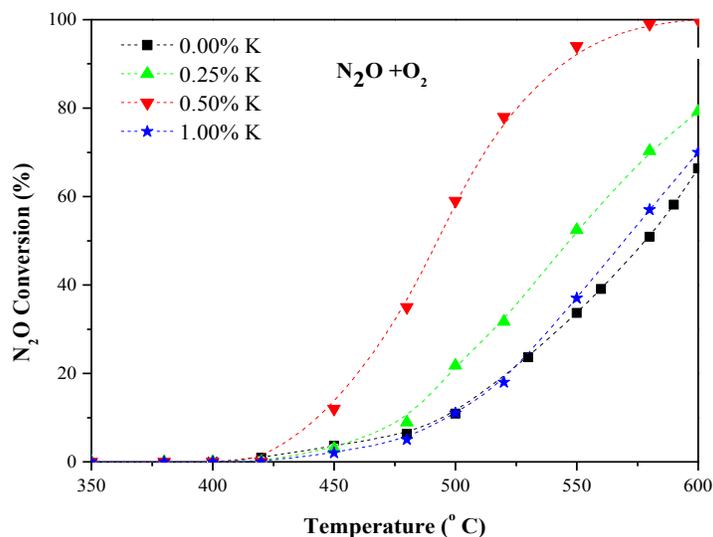

Figure 4. N$_2$O conversion over Ir(K)/Al$_2$O$_3$ catalysts in the presence of O$_2$ (GHSV: 40000h^{-1}, Feed: 0.1v/v% N$_2$O, 2v/v% O$_2$ diluted in He)

Figure 5 depicts the effect of alkali promotion on the light-off temperature (*i.e.*, the temperature required for 50% conversion of N$_2$O, T_{50}) for both reaction conditions (absence and presence of O$_2$). By comparing the two curves, it is evident that the de-N$_2$O behavior of Ir/Al$_2$O$_3$ catalyst under oxidizing conditions is remarkably enhanced by K addition while in the absence of oxygen the system is less sensitive to alkali promotion. Specifically, the optimum alkali-content (0.5 wt. %) offers a significant decrease of T_{50}, equal to $\Delta T = 80^{\circ}C$, under O$_2$ excess conditions, as compared to $\Delta T = 10^{\circ}C$ in the absence of oxygen.
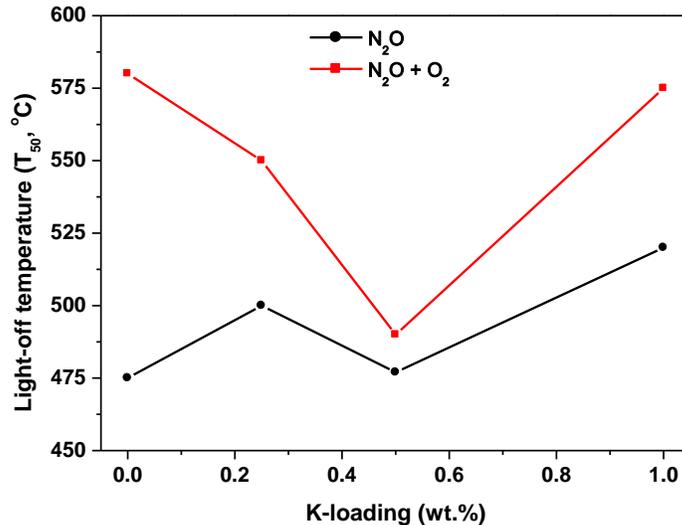
Figure 5. Effect of reaction conditions and K loading on the light-off temperature ($T_{50\%}$) of Ir/Al$_2$O$_3$ catalysts GHSV: 40000h^{-1}, Feed: 0.1v/v% N$_2$O and/or 2v/v% O$_2$ diluted in He)

On the light of the aforementioned findings it can be argued that K-addition has a beneficial effect on N$_2$O decomposition only under O$_2$ excess conditions. In opposite, the effect of alkali addition on N$_2$O conversion was detrimental in oxygen-free containing feed. These results can be interpreted by taking primarily into account the N$_2$O decomposition mechanism over Ir-based catalysts [36] in conjunction to the impact of potassium promoter on the local surface structure of Ir species.

N$_2$O chemisorption takes place at first on metal active sites, followed by molecular N$_2$ release and formation of adsorbed oxygen (O$_{ads}$) species (reaction R1). The desorption of oxygen ad-species, which is considered as the rate determining step, could proceed *via* the Langmuir-Hinshelwood (reaction R2) and/or the Eley-Rideal (reaction R3) type of mechanisms.

$$N_2O_{ads} \rightarrow N_2(g) + O_{ads} \tag{R1}$$

$$2O_{ads} \rightarrow O_2(g) \tag{R2}$$

$$N_2O(g) + O_{ads} \rightarrow N_2(g) + O_2(g) \tag{R3}$$

TPR results clearly indicated that potassium addition suppressed the reduction of iridium species, shifting their reduction to higher temperatures. In a similar manner, it was demonstrated by means of TG-MS analysis that alkali-doping drastically promotes the oxidation of Ir under oxidizing conditions [37]. It was estimated by H$_2$ pulses that the un-promoted Ir sample posses a fraction of about 20% IrO$_2$, in opposite to alkali-doped samples where the IrO$_2$ content was as high as 90% [37]. Moreover, King and co-workers showed by combining energetic data from density functional theory with thermodynamic calculations, that

under oxygen excess conditions the oxygen coverage in iridium surface is progressively built up, resulted eventually to the formation of IrO_2 [38].

Therefore, under oxygen deficient conditions, it can be argued that the catalyst surface is predominated by metallic iridium, in agreement to relevant studies [37]. These sites could be relatively active for N_2O decomposition, but progressively deactivated by the accumulation of surface oxygen ad-species. In opposite, the alkali-doping under oxygen excess conditions drastically promotes the oxidation of metallic Ir to IrO_2, in which the desorption of adsorbed oxygen species is facilitated [39]. Therefore, the pronounced effect of potassium under oxygen excess conditions can be attributed to the enhancement of N_2O adsorption and its concomitant dissociation (due to the increase of catalyst's surface basicity) as well as to the facilitation of oxygen desorption from IrO_2 sites. In this regard, the effect of alkali modifiers on the deN_2O performance should be always assessed in relation to the reaction conditions employed; alkali-doping in combination with oxygen excess conditions are required towards the formation of IrO_2 phase. In a similar manner, it has been reported that the activity of Ir-based catalysts is notably enhanced after high temperature treatment, which results to the establishment of a certain $Ir^{\delta+}/Ir^0$ ratio [40].

4 Conclusions

The impact of potassium loading (0-1.0 wt.% K) on the physicochemical characteristics and the de-N_2O performance of Ir/Al_2O_3 catalysts was investigated. The results revealed the pronounced effect of potassium under oxygen excess conditions (2v/v% O_2) with an optimal loading of 0.5 wt.% K. Complete conversion of N_2O was achieved at 550^oC over $Ir(K)/Al_2O_3$ catalyst, as compared to 30% over un-doped samples. In opposite, the de-N_2O performance was negatively affected upon increasing potassium loading under oxygen deficient conditions. The obtained results were interpreted on the basis of characterization results, which demonstrated an enhancement of the basic strength of catalyst surface as well as a strengthening in the Ir-O bond upon increasing potassium loading. Alkali-doping under oxygen excess conditions enhances the N_2O adsorption and its concomitant dissociation, whereas it promotes the formation of IrO_2, in which the desorption of adsorbed oxygen species is facilitated. Both factors operate together towards high N_2O decomposition rates under oxygen excess conditions.

References

1. Vitousek PM, Aber J, Howarth RW, Likens GE, Matson PA, Schindler DW, Schlesinger WH, Tilman GD (1997) Human alteration of the global nitrogen cycle: causes and consequences. Iss Ecol 1:1-17

2. Seinfeld JH, Pandis SN (1998) Atmospheric Chemistry and Physics. J. Wiley, New York

3. Huai T, Durbin TD, Miller JW, Norbeck JM (2004) Estimates of the emission rates of nitrous oxide from light-duty vehicles using different chassis dynamometer test cycles. Atmos Environ 38:6621-6629

4. Odaka M, Koike N, Suzuki H (2000) Influence of catalyst deactivation on N2O emissions from automobiles. Chemosphere—Glob Change Sci 2:413

5. Kapteijn F, Rodriguez-Mirasol J, Moulijn JA (1996) Heterogeneous catalytic decomposition of nitrous oxide. Appl Catal B: Environ 9:25-64

6. Burch R, Breen JP, Meunier FC (2002) A review of the selective reduction of NOx with hydrocarbons under lean-burn conditions with non-zeolitic oxide and platinum group metal catalysts. Appl Catal B: Environ 39:283-303

7. Konsolakis M, Drosou C, Yentekakis IV (2012) Support mediated promotional effects of rare earth oxides (CeO_2 and La_2O_3) on N_2O decomposition and N_2O reduction by CO or C_3H_6 over Pt/Al_2O_3 structured catalysts. Appl Catal B 123:405-413

8. Bueno-Lopez A, Such-Basanez I, Salinas-Martinez de Lecea C (2006) Stabilization of active Rh_2O_3 species for catalytic decomposition of N_2O on La-, Pr-doped CeO_2. J Catal 244:102-112

9. Konsolakis M, Aligizou F, Goula G, Yentekakis IV (2013) N_2O decomposition over doubly-promoted $Pt(K)/Al_2O_3$-$(CeO_2$-$La_2O_3)$ structured catalysts: On the combined effects of promotion and feed composition. Chem Eng J 230:286-295

10. Luo J, Gao F, Kim DH, Peden CHF (2014) Effects of potassium loading and thermal aging on $K/Pt/Al_2O_3$ high-temperature lean NOx trap catalysts. Catal Today 231:164-172

11. Pekridis G, Kaklidis N, Konsolakis M, Iliopoulou EF, Yentekakis IV, Marnellos GE (2011) Correlation of surface characteristics with catalytic performance of potassium promoted Pd/Al_2O_3 catalysts: The case of N_2O reduction by alkanes or alkenes. Top Catal 54:1135-1142

12. Okumura K, Motohiro T, Sakamoto Y, Shinjoh H (2009) Effect of combination of noble metals and metal oxide supports on catalytic reduction of NO by H_2. Surf Sci 603:2544-2550

13. Haber J, Nattich M, Machej T (2008) Alkali-metal promoted rhodium-on-alumina catalysts for nitrous oxide decomposition. Appl Catal B 77:278-283

14. Matsouka V, Konsolakis M, Lambert RM, Yentekakis IV (2008) In situ DRIFTS study of the effect of structure (CeO_2–La_2O_3) and surface (Na) modifiers on the catalytic and surface behaviour of Pt/γ-Al_2O_3 catalyst under simulated exhaust conditions. Appl Catal B: Environ 84:715-722

15. Brosda S, Vayenas CG (2006) Rules of chemical promotion. Appl Catal B: Environ 68:109–124

16. Koukiou S, Konsolakis M, Lambert RM, Yentekakis IV (2007) Spectroscopic evidence for the mode of action of alkali promoters in Pt-catalysed de-NOx chemistry. Appl Catal B 76:101-106

17. Maniak G, Stelmachowski P, Zasada F, Piskorz W, Kotarba A, Sojka Z (2011) Guidelines for optimization of catalytic activity of 3d transition metal oxide catalysts in N_2O decomposition by potassium promotion. Catal Today 176:369– 372

18. Stelmachowski P, Maniak G, Kotarba A, Sojka Z (2009) Strong electronic promotion of Co_3O_4 towards N_2O decomposition by surface alkali dopants, Catal Commun 10:1062–1065

19. Inger M, Kowalik P, Saramok M, Wilk M, Stelmachowski P, Maniak G, Granger P, Kotarba A, Sojka Z (2011) Laboratory and pilot scale synthesis, characterization and reactivity of multicomponent cobalt spinel catalyst for low temperature removal of N_2O from nitric acid plant tail gases. Catal Today 176:365– 368

20. Zasada F, Stelmachowski P, Maniak G, Jean-Francois P, Kotarba A, Sojka Z (2009) Potassium Promotion of Cobalt Spinel Catalyst for N_2O Decomposition—Accounted by Work Function Measurements and DFT Modelling. Catal Lett 127:126–131

21. Parres-Esclapez S, Lopez-Suarez FE, Bueno-Lopez A, Illan-Gomez MJ, Ura B, Trawczynski J (2009) Ph-Sr/Al_2O_3 catalyst for N_2O decomposition in the presence of O_2. Top Catal 52:1832-1836

22. Pekridis G, Kaklidis N, Konsolakis M, Athanasiou C, Yentekakis IV, Marnellos G (2011) A comparison between electrochemical and conventional catalyst promotion: the case of N2O reduction by alkanes or alkenes over K-modified Pd catalysts. Sol St Ion 192:653-658

23. Pachatouridou E, Papista E, Iliopoulou EF, Delimitis A, Goula G, Yentekakis IV, Marnellos GE, Konsolakis M (2015) Nitrous oxide decomposition over Al_2O_3 supported noble metals (Pt, Pd, Ir): Effect of metal loading and feed composition. J Environ Chem Eng 3:815-821

24. Travert A, Vimont A, Sahibed-Dine A, Daturi M, Lavalley J-C (2006) Use of pyridine CH(D) vibrations for the study of Lewis acidity of metal oxides. Appl Catal A 307:98

25. Lercher JA, Jentys A (2007) Infrared and raman spectroscopy for characterizing zeolites. Stud Surf Sci Catal 168:435

26. Emeis CA (1993) Determination of integrated molar extinction coefficients for infrared adsorption bands of pyridine adsorbed on solid acid catalysts. J Catal 141:347

27. Iliopoulou EF, Efthimiadis EA, Nalbandian L, Vasalos IA, Barth JO, Lercher JA (2005) Ir-based additives for NO reduction and CO oxidation in the FCC regenerator: Evaluation, characterization and mechanistic studies. Appl Catal B Environ 60:2277-288

28. Vicerich MA, Benitez VM, Especel C, Epron F, Pieck CL (2013) Influence of iridium content on the behaviour of Pt-Ir/ Al_2O_3 and Pt-Ir/ TiO_2 catalysts for selective ring opening of naphthenes, Appl Catal A Gen 453:167-174

29. Ding M, Tu J, Qiu M, Wang T, Ma L, Li Y (2015) Impact of potassium promoter on Cu-Fe based mixed alcohols synthesis catalyst. Appl Energ 138:584-589

30. Vernoux P, Leinekugel-LeCocq A-Y, Gaillard F (2003) Effect of the addition of Na to Pt/Al_2O_3 catalysts for the reduction of NO by C_3H_8 and C_3H_6 under lean-burn conditions. J Catal 219:247-257

31. Yentekakis IV, Tellou V, Botzolaki G. Rapakousios IA (2005) A comparative study of the C_3H_6+NO+O_2, C_3H_6+O_2 and NO+O_2 reactions in excess oxygen over Na-modified Pt/γ-Al_2O_3 catalysts Appl Catal B 56:229-239

32. Bruner E, Pfeifer H (2008) NMR Spectroscopic techniques for determining acidity and basicity. Mol Sieves 6:1-43

33. Damon JP, Scokart PO (1980) Acid-base Properties of Alkali Promoted Chromia-alumina Catalysts. Chem Lett 3:327-330

34. Abello MC, Gomez MF, Cadus LE (1998) Selective oxidation of propane on MgO/-Al$_2$O$_3$-supported molybdenum catalyst: influence of promoters. Catal Lett 53:185-192

35. Wang Y, Liu HH, Wang SY, Luo MF, Lu JQ (2014) Remarkable enhancement of dichloromethane oxidation over potassium-promoted Pt/Al$_2$O$_3$ catalysts. J Catal 311:314-324

36. Shen Q, Li L, Hao Z, Xu ZP (2008) Highly active and stable bimetallic Ir/Fe-USY catalysts for direct and NO-assisted N$_2$O decomposition. Appl Catal B: Environ 84:734-741

37. Wögerbauer C, Maciejewski M, Schubert MM, Baiker A (2001) Effect of sodium on the catalytic properties of iridium black in the selective reduction of NO$_x$ by propene under lean-burn conditions. Catal Lett 74:1–7

38. Liu ZP, Jenkins JS, King DA (2004) Car Exhaust Catalysis from First Principles: Selective NO Reduction under Excess O$_2$ Conditions on Ir. J Am Chem Soc 126:10747

39. Bueno-López A, Such-Basáñez I, Salinas-Martínez de Lecea C (2006) Stabilization of active Rh$_2$O$_3$ species for catalytic decomposition of N$_2$O on La-, Pr-doped CeO$_2$. J Catal 244:102–112

40. Amiridis MD, Mihut C, Maciejewski M, Baiker A (2001) The selective catalytic reduction of NO by hydrocarbons over Pt- and Ir-based catalysts. Top Catal 28:141-150